

## Inactivations of *rsbU* and *sarA* by IS256 Represent Novel Mechanisms of Biofilm Phenotypic Variation in *Staphylococcus epidermidis*

Kevin M. Conlon, Hilary Humphreys, and James P. O’Gara\*

Department of Microbiology, RCSI Education and Research Centre, Beaumont Hospital, Royal College of Surgeons in Ireland, Dublin, Ireland

Received 8 March 2004/Accepted 10 June 2004

**Expression of *ica* operon-mediated biofilm formation in *Staphylococcus epidermidis* RP62A is subject to phase variable regulation. Reversible transposition of IS256 into *icaADBC* or downregulation of *icaADBC* expression are two important mechanisms of biofilm phenotypic variation. Interestingly, the presence of IS256 was generally associated with a more rapid rate of phenotypic variation, suggesting that IS256 insertions outside the *ica* locus may affect *ica* transcription. Consistent with this, we identified variants with diminished *ica* expression, which were associated with IS256 insertions in the  $\sigma^B$  activator *rsbU* or *sarA*. Biofilm development and *ica* expression were activated only by ethanol and not NaCl in *rsbU*::IS256 insertion variants, which were present in ~11% of all variants.  $\sigma^B$  activity was impaired in *rsbU*::IS256 variants, as evidenced by reduced expression of the  $\sigma^B$ -regulated genes *asp23*, *csb9*, and *rsbV*. Moreover, expression of *sarA*, which is  $\sigma^B$  regulated, and SarA-regulated RNAPIII were also suppressed. A biofilm-forming phenotype was restored to *rsbU*::IS256 variants only after repeated passage and was not associated with IS256 excision from *rsbU*. Only one *sarA*::IS256 insertion mutant was identified among 43 biofilm-negative variants. Both NaCl and ethanol-activated *ica* expression in this *sarA*::IS256 variant, but only ethanol increased biofilm development. Unlike *rsbU*::IS256 variants, reversion of the *sarA*::IS256 variant to a biofilm-positive phenotype was accompanied by precise excision of IS256 from *sarA* and restoration of normal *ica* expression. These data identify new roles for IS256 in *ica* and biofilm phenotypic variation and demonstrate the capacity of this element to influence the global regulation of transcription in *S. epidermidis*.**

Biofilm formation by staphylococci on implanted biomaterials is now recognized as an important virulence factor contributing to the development of a significant proportion of all device-related infections. Enzymes encoded by the *icaADBC* operon (20, 23, 27) are required for synthesis of an extracellular polysaccharide termed polysaccharide intercellular adhesin (PIA) in *Staphylococcus epidermidis* (37, 58) and poly-*N*-acetylglucosamine (PNAG) in *S. aureus* (12, 31, 41, 43, 44), which plays an important role in both the initial attachment and cellular proliferation processes characteristic of staphylococcal biofilm development (27, 38, 38, 40).

Much effort has been focused on understanding the regulation of *ica* operon expression, and it is now known that increased transcription of the *ica* operon can be observed under anaerobic growth conditions (13), in the presence of subinhibitory concentrations of certain antibiotics, and in response to osmotic stress (32, 52). We have recently reported that the *icaR* gene encodes a transcriptional repressor with a central role in the environmental regulation of *ica* operon expression in *S. epidermidis* (10, 11). Jefferson et al. (29) demonstrated that purified IcaR protein from *S. aureus* bound the *ica* operon promoter region close to the *icaA* start codon. Consistent with this, deletion of the *icaR* gene in *S. aureus* is also associated with activation of *ica* operon expression (30; C. A. Kennedy and J. P. O’Gara, unpublished data). A new negative regulator of *ica* operon expression, the teicoplanin-associated locus reg-

ulator (TcaR), has also been recently described in *S. aureus* (30).

The *S. aureus* global stress response regulator,  $\sigma^B$ , and the *S. epidermidis* *rsbU* gene (a positive regulator of  $\sigma^B$ ) have also been implicated in the regulation of biofilm development in *S. aureus* and *S. epidermidis* (32, 51). Interestingly, induction of biofilm by NaCl is affected in *S. epidermidis* *rsbU* and *S. aureus*  $\sigma^B$  mutants (32, 51). However, the role of  $\sigma^B$  in the regulation of *ica* operon expression remains unclear given the absence of an identifiable consensus binding site for this sigma factor upstream of the *icaA* or *icaR* start codons. In addition, Valle et al. (54) recently reported that the staphylococcal accessory regulator, *sarA*, which controls the expression of over 100 genes (16), and not  $\sigma^B$  was required for *ica* operon expression, PIA/PNAG synthesis, and biofilm development in *S. aureus*, although  $\sigma^B$  was found to influence the regulation of *ica* operon transcription. In contrast, a transposon mutation in the *rsbU* gene in *S. epidermidis* was associated with both a reduction in PIA/PNAG levels and the loss of biofilm-forming capacity (32).

Coagulase-negative staphylococci and *S. aureus* are capable of rapid phenotypic switching involving properties such as colony morphology, growth rate, antibiotic susceptibility, and biofilm-forming capacity (9, 11, 14, 25, 45, 46, 58, 59). In terms of pathogenesis, staphylococcal phenotypic variation may contribute to dissemination, invasive disease, and sepsis. Ziebuhr et al. (59) demonstrated that reversible inactivation of the *ica* operon by the insertion sequence element IS256 can result in the production of 25 to 33% of phenotypic variants. More recently, we characterized multiple *S. epidermidis* isolates and demonstrated that downregulation of *ica* operon expression

\* Corresponding author. Mailing address: Department of Microbiology, RCSI Education and Research Centre, Beaumont Hospital, Royal College of Surgeons in Ireland, Dublin 9, Ireland. Phone: 353-1-809-3711. Fax: 353-1-809-3709. E-mail: jogara@rcsi.ie.

TABLE 1. Rate of phenotypic switching in IS256-positive and IS256-negative clinical isolates of *S. epidermidis*

<i>S. epidermidis</i> strain	Relevant characteristic(s)	IS256	Avg ON-to-OFF switching rate (SD) <sup>a</sup>	Source or reference
RP62A	Biofilm-positive, blood culture isolate	+	5.5 (1.4) × 10 <sup>-5</sup>	ATCC 35984 <sup>b</sup>
CSF24047	Biofilm-positive, blood culture isolate (Beaumont Hospital, Dublin, Ireland)	+	5.3 (2.5) × 10 <sup>-5</sup>	This study
13652	Biofilm-positive, blood culture isolate (Duke University, Durham, NC.)	+	4.1 (1.6) × 10 <sup>-5</sup>	Vance Fowler, Duke University
17174	Biofilm-positive, blood culture isolate (Duke University, Durham, NC.)	+	4.4 (2.3) × 10 <sup>-5</sup>	Vance Fowler, Duke University
8621	Biofilm-positive, blood culture isolate (Duke University, Durham, NC.)	+	3.0 (0.5) × 10 <sup>-5</sup>	Vance Fowler, Duke University
SE56	Biofilm-positive, blood culture isolate (Medical College of Virginia, Richmond, Va.)	+	3.2 (1.0) × 10 <sup>-5</sup>	Paul Fey, University of Nebraska
CSF41498	Biofilm-positive, cerebrospinal fluid isolate	-	0.17 (0.02) × 10 <sup>-5</sup>	11
SE5	Biofilm-positive, blood culture isolate (Medical College of Virginia, Richmond, Va.)	-	0.15 (0.06) × 10 <sup>-5</sup>	Paul Fey, University of Nebraska (53)
1457	Biofilm-positive, blood culture isolate (Hamburg, Germany)	-	1.3 (0.6) × 10 <sup>-5</sup>	D. Mack, Hamburg, Germany
BC78032	Biofilm-positive, blood culture isolate (Beaumont Hospital, Dublin, Ireland)	-	0.87 (0.55) × 10 <sup>-5</sup>	This study
BC78037	Biofilm-positive, blood culture isolate (Beaumont Hospital, Dublin, Ireland)	-	0.76 (0.23) × 10 <sup>-5</sup>	This study
14765	Biofilm-positive, blood culture isolate (Duke University, Durham, NC.)	-	1.0 (0.7) × 10 <sup>-5</sup>	Vance Fowler, Duke University

<sup>a</sup> That is, the rate of biofilm-positive to biofilm-negative switching per CFU per generation. Assays were performed on at least three independent occasions for each strain. Average values and standard deviations are shown.

<sup>b</sup> ATCC, American Type Culture Collection.

and mutation are the primary mechanisms responsible for biofilm phenotypic variation (25). It therefore appears that more than one mechanism contributes to the production of phenotypic variants in *S. epidermidis*. In this context, it is interesting to note the reported association between the levels of resistance to methicillin, oxacillin, and penicillin and biofilm-forming capacity in phenotypic variants of *S. epidermidis* (45, 46), suggesting that the phenotypic switch associated with impaired biofilm-forming capacity may also impact on other properties. In addition, the global regulators Agr and SarA, which influence methicillin resistance in *S. aureus* (50), have also been demonstrated to regulate staphylococcal biofilm formation (2, 54, 56, 57).

In the present study we characterized the contribution of IS256 to the production of biofilm-negative variants with diminished *ica* operon expression. Two genetic switches were identified that involved IS256 insertions at the *rsbU* and *sarA* genes. The impact of IS256 insertions in both genes on biofilm,  $\sigma^B$  regulon, and *agr* and *sarA* expression was examined. The data presented here provide new insights into biofilm phenotypic variation and the impact of IS256-mediated dynamic genetic events on the activity of at least three global regulators and the regulation of staphylococcal biofilm formation.

#### MATERIALS AND METHODS

**Bacterial strains, media, growth conditions, and isolation of biofilm-negative phenotypic variants.** The bacterial strains used in the present study are shown in Table 1. Bacteria were routinely grown at 37°C on brain heart infusion (BHI) medium (Oxoid) supplemented with 4% ethanol, 4% NaCl, or 10% NaCl. Semi-quantitative determinations of biofilm formation in 96-well tissue culture plates (Nunc) were performed as described previously (11). To screen for biofilm-negative phenotypic variants bacteria were grown on Congo red agar (CRA) plates as described previously (10, 11, 59).

**Measurement of biofilm phase variation (switching) rates.** To examine the rates of phenotypic switching, we adapted the method of Eisenstein (17) as

described previously (48) to measure the rate at which variant cells were produced during the growth of a colony from a single biofilm-forming CFU. Black colonies from CRA were restreaked onto BHI agar and incubated overnight at 37°C. Individual colonies from these plates, which are almost exclusively derived from an initially biofilm-positive CFU, were resuspended and serially diluted in sterile H<sub>2</sub>O, plated onto CRA plates, and incubated at 37°C for 24 h. Plates were inspected by using a colony microscope to identify and count the number of variant colonies as a proportion of the total number of parental, biofilm-positive, black colonies, which in turn reflects the proportion of variant and parental cells in the original colony. Since each biofilm-positive colony analyzed in this way originates from a biofilm-positive bacterial CFU, the proportion of bacterial cells that have switched to the variant phenotype in the resulting colony is a reflection of the phenotypic switching rate. The number of generations required for an individual biofilm-positive CFU to give rise to a colony is calculated by dividing the log of the total viable count by the log of 2 [i.e., log(total viable count)/log(2)]. The data were recorded as phenotypic switch frequencies per CFU per generation.

**Isolation of biofilm-positive revertants.** A single colony of a biofilm-negative phenotypic variant was grown in BHI medium at 37°C in a tissue culture flask. After 24 h the medium was replaced. This procedure was repeated until a biofilm of adhering bacteria became visible on the bottom of the tissue culture flask or at the liquid-air interface (minimum of 4 days). After a wash with phosphate-buffered saline (PBS), the adhering bacterial cells were scratched from the bottom and streaked on CRA. After incubation at 37°C overnight and an additional 24 h at room temperature, single, black colonies were isolated.

**Genetic techniques.** Genomic and plasmid DNA purification and manipulations were performed as described previously (10, 11). The oligonucleotide primers used in the present study were supplied by MWG Biotech (Germany) and are listed in Table 2.

The primers ICAR1 and ICAC1 were used to amplify a 4,204-bp fragment comprising the entire *ica* operon under the following conditions: 35 cycles of 94°C for 30 s, 47°C for 30 s, and 72°C for 5 min. The primers PV1 and PV2 were used to amplify an 871-bp product comprising the *icaR* gene and the *ica* operon promoter region under the following conditions: 35 cycles of 94°C for 30 s, 50°C for 30 s, and 72°C for 1 min.

Amplification of a 3,910-bp fragment encompassing the *rsbU*, *rsbV*, *rsbW*, and *sigB* genes was achieved by using the primers SEsigFor and SEsigRev under the following conditions: 35 cycles of 94°C for 30 s, 55°C for 30 s, and 72°C for 5 min. The primers rsbUFor and rsbU2 were used to amplify a 240-bp product comprising an internal portion at the 5' end of the *rsbU* gene under the following

TABLE 2. Oligonucleotide primers used in this study

Target gene(s)	Primers	Primers sequence (5'-3')
<i>rsbU</i> , <i>rsbV</i> , <i>rsbW</i> , <i>sigB</i>	SESigFor SESigRev	TCACCAGTTCAAGGGTCTGA TCTTTGGAGCTTCGTCTGTG
<i>icaR</i> , <i>icaADBC</i>	ICAR1 ICAC1	CTCGAATTTGTTACATACTAG CCATAGCTTGAATAAGGGAC
<i>icaR</i> , <i>ica</i> operon promoter	PV1 PV2 rsbUVFor rsbUVRev	TTTGAAATCTCGAATTTGTTACAT CAATGATCGATTAAGGGTTTTTTC GGAAGTAAGGAGGCGCATT GCGCCAGCTCTTAAAAATAC
<i>rsbU</i> , <i>rsbV</i>	rsbUFor rsbU2 rsbU4 rsbU5	GGAAGTAAGGAGGCGCATT CGACTTCTGGTAACACATCGAG AAAATTTGGCATGGATGCTT CGTCCAATCTCCACCAACT
<i>asp23</i>	SEasp23For SEasp23Rev	CATGAAAGGTGGCTTCACAG CATTACGTCGTCAACTTGCAT
<i>csb9</i>	SEcsb9For SEcsb9Rev	ATTCGATGCGAGTGGAGATT CGTGGAATTGATCCTGCTTT
<i>rsbV</i>	SersbVFor SersbVRev	TTGGTGGAGAATTGGACGTA CCTATCCGCTCTGAAACACC
<i>RNAIII</i>	SERNAIIFor SERNAIIRRev SEsarAFor SEsarARev	TGAAGTTATGATGGCAGCAGAT GTTGGGATGGCTCAACAAC TCAGCTTTGAAGAAATTTGCAG TCTTTCATCGTGTTCATTACGTTT
<i>sarA</i>	SEsarA1 SEsarA2 SEsarA3 SEsarA4	TCCCTTCAAAAACCAAACGAA AATTCAGGACATGCACCACA AAAAGATGGGTTTTAAGATTTATGGA CTGTCCAGCATAAGTGACCATAGC
<i>icaA</i>	KCA1 KCA2	AACAAGTTGAAGGCATCTCC GATGCTTGTATTCCCT
<i>icaR</i>	KCR1 KCR2	GGTAAAGTCCGTCATGGAA CGCAATAACCTTATTTTCCG
<i>gyrB</i>	GYR1 GYR2	TTATGGTGCTGGACAGATACA CACCGTGAAGACCGCCAGATA

conditions: 35 cycles of 94°C for 30 s, 50°C for 30 s, and 72°C for 1 min. The primers rsbUVFor and rsbUVRev were used to amplify a 1,552-bp product comprising the *rsbU* and *rsbV* genes under the following conditions: 35 cycles of 94°C for 30 s, 50°C for 30 s, and 72°C for 1 min.

The *sarA* locus was amplified on a 1,498-bp fragment by using the primers SEsarA1 and SEsarA2 under the following conditions: 35 cycles of 94°C for 30 s, 55°C for 30 s, and 72°C for 2 min.

*S. epidermidis* strains were screened for the presence of IS256 by using a PCR assay as described previously (11).

Nucleotide sequencing was performed commercially by MWG Biotech (Germany) with the following primers: rsbUFor, rsbU2, rsbU4, rsbU5, SEsarAFor, SEsarARev, PV1, and PV2.

**RNA purification and RT-PCR.** RNA purification, reverse transcription-PCR (RT-PCR) and analysis of RT-PCR data was performed as described previously (10, 11), with the following oligonucleotide primer pairs: GYR1 and GYR2 (*gyrB*), KCA1 and KCA2 (*icaA*), KCR1 and KCR2 (*icaR*), SEasp23For and SEasp23Rev (*asp23*), SEcsb9For and SEcsb9Rev (*csb9*), SersbVFor and SersbVRev (*rsbV*), SEsarAFor and SEsarARev or SEsarA3 and SEsarA4 (*sarA*), and SERNAIIFor and SERNAIIRRev (RNAIII). RT was performed at 55°C for 30 min, followed by 14 to 24 amplification cycles of 94°C 30 s, 50°C 30 s, and 72°C 30 sec.

**Hemagglutination assays.** PIA/PNAG expressed by *S. epidermidis* strains has been shown to be responsible for their ability to agglutinate red blood cells (18,

31, 39). Thus, the hemagglutination assay can be used as an indirect assay for PIA/PNAG production. Briefly, *S. epidermidis* RP62A cultures were grown to early stationary phase (optical density at 600 nm [OD<sub>600</sub>] = 6.0) in BHI medium. A 1% sheep red blood (SRB) cell suspension was made by reconstituting lyophilized SRB cells (Sigma, St. Louis, Mo.) in PBS supplemented with 1% bovine serum albumin. The bacterial cultures were washed once in PBS and resuspended in PBS supplemented with an additional 2% NaCl. Then, 50 µl of the cell suspension was added to each well in the top row of a round-bottom 96-well plate, and subsequent twofold dilutions were made in PBS supplemented with an additional 2% NaCl. Subsequently, a 50-µl aliquot of 1% SRB was added to each well, and the plate was incubated without mixing at room temperature for 2 h before visual examination. A positive result was defined as the production of diffuse red blood cells with no red blood cells pelleting at the bottom of the well.

## RESULTS

**Contribution of IS256 to biofilm phenotypic switching.** A role for IS256 in phenotypic variation of biofilm formation in *S. epidermidis* was originally described by Ziebuhr et al. (58). Insertional inactivation of the *ica* operon by this mobile genetic element via a unique and reversible mechanism results in the

production of between 25 and 33% of phenotypic variants in the reference strain RP62A (59). More recently, we conducted an analysis of multiple *S. epidermidis* isolates which suggested that mutation and downregulation of *ica* operon expression are the primary mechanisms governing biofilm phenotypic variation (25).

To further investigate biofilm phenotypic variation in *S. epidermidis* strains, we measured the rate of phenotypic switching in six strains harboring IS256 (RP62A, CSF24047, SE56, 13652, 8621, and 17174) and six strains lacking IS256 (CSF41498, SE5, 14765, 1457, BC78032, and BC70837) (Table 1). To facilitate this analysis, we adapted the method of Eisenstein (17) as described previously (48) to measure the rate at which variant cells were produced during the growth of a colony from a biofilm-forming CFU (Materials and Methods). The data are expressed as the rate of switching per CFU per generation. To assess the validity of this methodology, we confirmed that rate of phenotypic switching for *S. epidermidis* RP62A was ca.  $5.5 \times 10^{-5}$  per cell per generation, which was in good agreement with previous measurements for this strain (59).

Similar to RP62A, the biofilm-positive to biofilm-negative switching frequencies in the five clinical isolates that harbor the IS256 element (CSF24047, 13652, 8621, 17174, and SE56) were between  $3 \times 10^{-5}$  and  $5.5 \times 10^{-5}$  per CFU per generation (Table 1). In contrast, the switching frequencies in the six IS256-negative isolates were significantly reduced compared to the IS256-positive strains ( $P = 1.8 \times 10^{-5}$ ) (Table 1). This low switching frequency in the IS256-negative strains also contrasted with the switching frequencies reported by others in both *S. epidermidis* (58) and *S. aureus* (1), all of which were ca.  $10^{-5}$  per cell per generation. These data suggest that the presence of IS256 is generally associated with more rapid phenotypic variation of biofilm-forming capacity in *S. epidermidis*.

**Regulation of *ica* operon expression and biofilm formation in a phenotypic variant of *S. epidermidis* RP62A.** To investigate the possibility that IS256 insertions outside the *ica* operon may play a role in the more rapid production of biofilm-negative variants with reduced *ica* operon transcription, we characterized the environmental regulation of *ica* operon expression in biofilm-negative variants of RP62A. RT-PCR was used to measure *icaA* and *icaR* transcription in variants grown in BHI broth or BHI medium supplemented with 4% NaCl, 10% NaCl, or 4% ethanol. This analysis revealed that growth of one variant, designated 33A, in the presence of 4% ethanol but not in the presence of 4% or 10% NaCl resulted in *ica* operon activation (Fig. 1A). Consistent with this, at the phenotypic level, the capacity of 33A to form biofilm was partially restored (albeit not to wild-type levels) in the presence of ethanol but not NaCl (Fig. 1B). Interestingly, Knobloch et al. (32) also reported that a transposon mutation in the *rsbU* gene of *S. epidermidis* 1457 resulted in a biofilm-negative phenotype, which could be reversed by growth in ethanol but not NaCl. *rsbU* is the first gene of the *sigB* operon and encodes a phosphatase, which positively regulates  $\sigma^B$  (32). Using RT-PCR we demonstrated that, a finding consistent with the biofilm phenotypes, growth of the 1457 *rsbU* transposon mutant M15 only in ethanol and not NaCl was associated with activation of *ica* operon expression (Fig. 1C and D). In addition, because PIA/PNAG expressed by *S. epidermidis* strains mediates erythrocyte

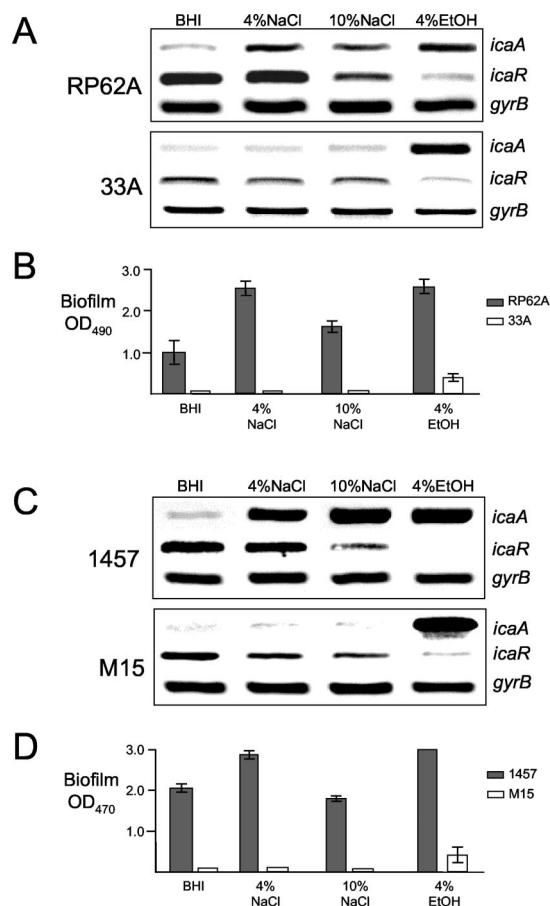


FIG. 1. Characterization of *S. epidermidis* RP62A, 33A, 1457, and M15 genotypes and phenotypes. (A) Comparative measurement of *icaA*, *icaR*, and *gyrB* (control) transcription in RP62A and 33A. RT-PCR analysis was performed on RNA prepared from cultures grown at 37°C to an OD<sub>600</sub> of 4.0 in BHI medium or BHI medium supplemented with 4% NaCl, 10% NaCl, or 4% ethanol. (B) Biofilm formation in tissue culture treated 96-well plates by RP62A and 33A in BHI medium or BHI medium supplemented with 4% NaCl, 10% NaCl, or 4% ethanol. (C) Comparative measurement of *icaA*, *icaR*, and *gyrB* (control) transcription in 1457 and M15. RT-PCR analysis was performed on RNA prepared from cultures grown at 37°C to an OD<sub>600</sub> of 4.0 in BHI medium or BHI medium supplemented with 4% NaCl, 10% NaCl, or 4% ethanol. (D) Biofilm formation in tissue culture treated 96-well plates by RP62A and 33A in BHI medium or BHI medium supplemented with 4% NaCl, 10% NaCl, or 4% ethanol. Biofilm values represent OD<sub>490</sub> readings after staining with crystal violet and are the means of at least three independent assays. Standard deviations are indicated where applicable. EtOH, ethanol.

agglutination (18, 31, 39), the ability of 33A to agglutinate SRB cells was tested. Consistent with the reduced levels of *ica* operon transcription, hemagglutination assays revealed a significant reduction in PIA/PNAG levels in 33A compared to RP62A (data not shown). These data suggested that altered  $\sigma^B$  activity in the RP62A variant 33A may be responsible for diminished *ica* operon expression and the biofilm-negative phenotype.

**Analysis of  $\sigma^B$  activity in phenotypic variants.** In order to assess the levels of  $\sigma^B$  activity in the RP62A variant 33A, we used RT-PCR to measure  $\sigma^B$ -dependent gene expression.

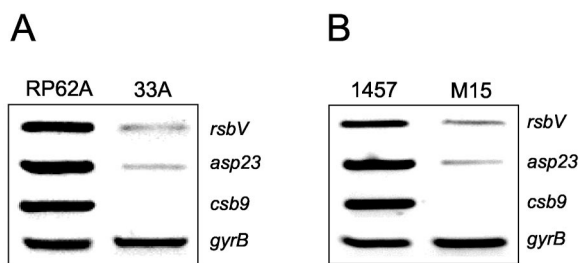


FIG. 2. Comparative measurement of *rsbV*, *asp23*, *csb9*, and *gyrB* (control) transcription in RP62A and 33A (A) and 1457 and M15 (B). RT-PCR analysis was performed on RNA prepared from cultures grown at 37°C to an OD<sub>600</sub> of 4.0 in BHI medium.

Three  $\sigma^B$ -regulated genes were chosen for this analysis: *asp23* (21, 34, 47, 51), *csb9* (22), and *rsbV* (24, 32, 49).

This analysis revealed that transcription of the *asp23*, *csb9*, and *rsbV* genes in the RP62A variant 33A were substantially reduced compared to the wild-type parent (Fig. 2A). In addition, a similarly dramatic decrease in *asp23*, *csb9*, and *rsbV* expression was observed in the *S. epidermidis* *rsbU* transposon mutant M15 compared to its wild-type parent 1457 (Fig. 2B). These findings strongly suggest that  $\sigma^B$  activity is impaired in variant 33A and that this change in the activity of a global regulator is responsible for diminished *ica* operon expression and a biofilm-negative phenotype.

**PCR amplification and nucleotide sequence analysis of the *sigB* locus from biofilm-negative variants.** Analysis of *ica* operon environmental regulation and  $\sigma^B$ -dependent gene expression in the RP62A variant 33A suggested that impaired  $\sigma^B$  activity may be responsible for the biofilm-negative phenotype. We therefore decided to characterize the *sigB* operon of variant 33A. The *sigB* operon of *S. epidermidis* has previously been characterized and comprises the four genes *rsbU*, *rsbV*, *rsbW*, and *sigB* (32). Long-range PCR amplification of the *sigB* operon generated products of ca. 5,200-bp for variant 33A compared to the expected size of 3,910 bp for RP62A (data not shown). This observation suggested that a genetic rearrangement may have occurred at the *sigB* locus of variant 33A and was particularly interesting given that IS256 insertions in the *ica* operon can also generate biofilm-negative variants (59). Restriction enzyme and nucleotide sequence analysis subsequently revealed the presence of an IS256 insertion at the 5' end of the *rsbU* gene in variant 33A and thus identified the genetic basis for the impaired  $\sigma^B$  activity in this strain (Fig. 3). Consistent with the findings of Ziebuhr et al. (59), the IS256 element, which was oriented in the opposite transcriptional orientation to the *rsbU* gene, was flanked by an 8-bp duplicated target sequence (Fig. 3).

**Frequency of *rsbU*::IS256 insertion variant production.** To determine the frequency at which *rsbU*::IS256 insertions occurred, we performed three independent experiments to isolate 43 biofilm-negative variants from RP62A. PCR analysis of all 43 variants revealed that 11 (25.5%) contained *ica*::IS256 insertions, whereas 5 (11.6%) contained IS256 insertions in the *rsbU* gene of the *sigB* locus. Nucleotide sequence analysis confirmed the presence of IS256 insertions in the *rsbU* gene and identified two new IS256 insertion sites at the 5' end of *rsbU* in four of these variants, which were designated Red 1, Red 2,

Red 3, and Red 4 (Fig. 3). The fifth variant, Red 5, contained an IS256 insertion at the 3' end of the *rsbU* gene (Fig. 3). In contrast to the IS256 insertion in variant 33A, IS256 was oriented in the same transcriptional orientation to the *rsbU* gene in all five of these variants. Similar to 33A, we identified 8-bp duplicated IS256 target sequences in all five of these *rsbU*::IS256 insertion variants; however, no consensus target sequence could be identified. These data suggest that the *rsbU* gene, and in particular the 5' end of this gene, may represent a chromosomal hot spot for IS256 insertions.

Seventeen phenotypic variants isolated from one experiment were characterized further by using PCR to amplify the *ica* and *sigB* operons and RT-PCR to measure *ica* operon and *asp23* expression (Fig. 4). In this particular experiment, 3 of the 17 variants examined were found to contain IS256 insertions in the *rsbU* gene of the *sigB* operon (Fig. 4A). Only one variant contained an *ica*::IS256 insertion (Fig. 4B), indicating that considerable variation in the rates of IS256 insertions at specific loci exists between experiments. Interestingly, RT-PCR analysis revealed that *ica* operon expression was substantially reduced in 14 of the 17 variants, including the three variants with *rsbU*::IS256 insertions (Fig. 4C). Importantly, five variants including the three *rsbU*::IS256 insertion variants were found to have reduced levels of *asp23* expression (Fig. 4C). The molecular basis for reduced *asp23* expression in the two variants that do not contain IS256 insertions in the *sigB* operon is unknown.

**Selection and analysis of biofilm-positive revertant strains from an *rsbU*::IS256 insertion variant.** Ziebuhr et al. (59) reported previously that biofilm-negative *icaC*::IS256 insertion variants were capable of reverting, after repeated passage, to a biofilm-positive phenotype after the complete excision of the insertion sequence element. In order to determine whether *rsbU*::IS256 insertion variants could also revert to a biofilm-positive phenotype, we serially passaged variant 33A in a tissue culture flask for up to 15 days. Seven independent flasks were used and revertants, which were isolated from a weak biofilm of adhering bacteria formed after 5 to 9 days, were identified as displaying a stable, black colony morphology on CRA. Interestingly, PCR revealed that in all revertants tested, the *rsbU*::IS256 insertion remained intact, suggesting that a secondary or compensatory mutation was responsible for the reversion to a biofilm-positive phenotype. To further investigate this possibility, we examined the *ica* operon and *asp23* gene expression in three revertants, 33A/1 to 33A/3. Consistent with the presence of an *rsbU*::IS256 allele, *asp23* expression levels were substantially lower in 33A, and all three revertants compared to wild-type RP62A (Fig. 5). In contrast, *ica* operon expression levels were predictably higher in all revertants compared to 33A but were not comparable to the levels of *ica* expression in RP62A (Fig. 5). Semiquantitative biofilm assays revealed that the revertant strains were only weakly biofilm positive when grown in BHI broth but were strongly biofilm positive when grown in NaCl or ethanol (data not shown). Thus, the biofilm phenotype of these revertants was different from both 33A and wild-type RP62A. We have previously reported that the *icaR* gene encodes a negative regulator involved in the environmental regulation of *ica* operon expression (10, 11). In order to determine whether mutations in the *ica* operon regulatory regions were responsible for the in-

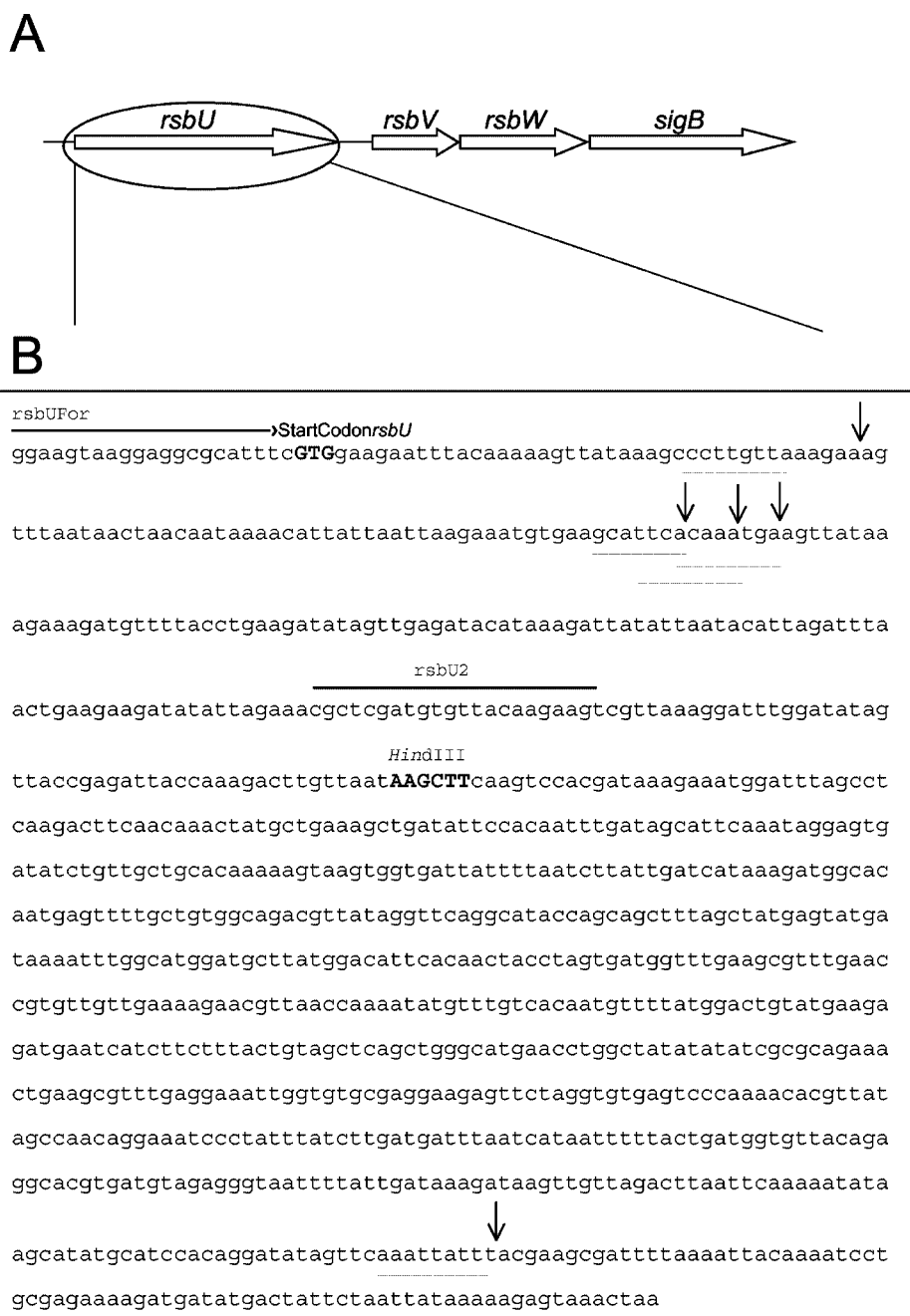


FIG. 3. Location of IS256 insertions in the *rsbU* gene. (A) Diagrammatic representation of the *rsbU*, *rsbV*, *rsbW*, *sigB* operon structure in *S. epidermidis*. (B) Exact locations of IS256 insertions detected in the *rsbU* gene of RP62A variants. The nucleotide binding sites for the PCR primers *rsbU*For and *rsbU*2, the *rsbU* start codon, and the location of a unique HindIII site are all indicated. The duplicated 8-bp IS256 target sequences—TTAAAGAA for Red 1; AGCATTCA for 33A; CAAATGAA for Red 2, Red 3, and Red 4; and AATTATTT for Red 5—are underlined, and arrows indicate the exact insertion sites.

creased levels of *ica* operon expression in the revertant strains, we determined the nucleotide sequence of the *icaR* gene and *ica* operon promoter region in all seven revertants. However, no sequence differences were identified in the *icaR* gene and *ica* operon promoter region of these revertants (data not shown).

**Impact of *rsbU*::IS256 insertions on the expression of *sarA* and *agr*.** The absence of a recognizable  $\sigma^B$  promoter upstream

of the *ica* operon (32, 51) may suggest an indirect role for  $\sigma^B$  in the regulation of *ica* operon transcription. In addition, Valle et al. (54) and Beenken et al. (2) recently demonstrated an essential role for the staphylococcal accessory regulator SarA in *S. aureus* biofilm development. Valle et al. (54) also demonstrated that inactivation of *sigB* in *S. aureus* was only associated with slightly decreased *ica* operon expression. Because  $\sigma^B$ -dependent promoters have been identified upstream of the

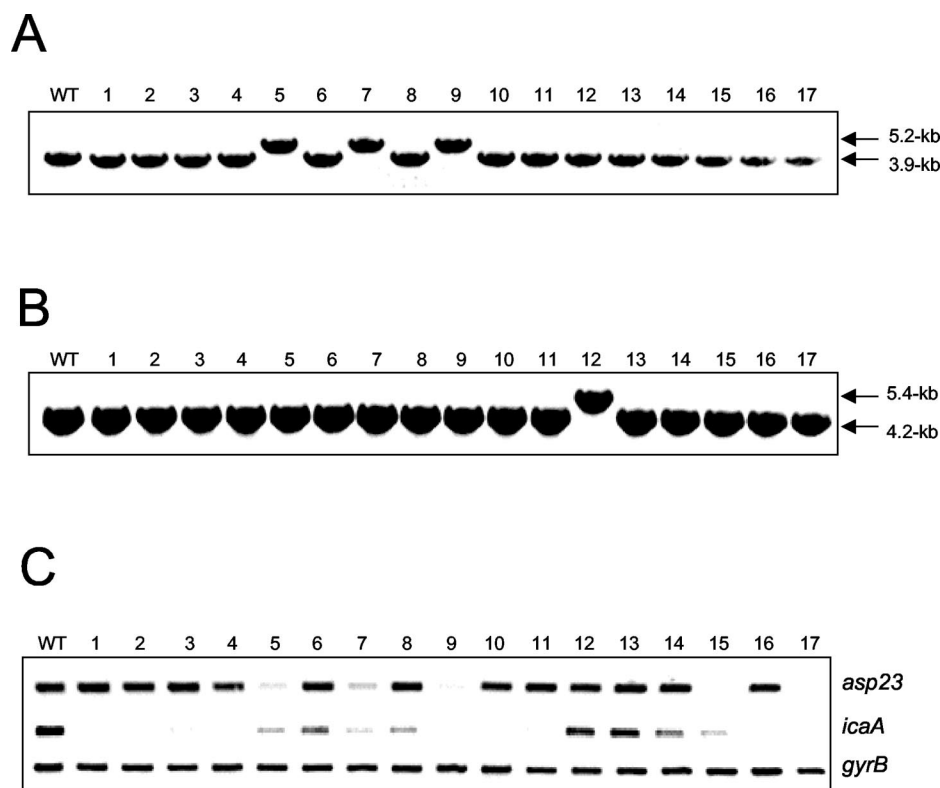


FIG. 4. Analysis of 17 phenotypic variants produced by *S. epidermidis* RP62A. (A and B) Long-range PCR analysis of the *sigB* operon (A) and *ica* operon (B) in the wild-type RP62A and in 17 phenotypic variants. (C) Comparative measurement of *asp23*, *icaA*, and *gyrB* (control) transcription in wild-type RP62A and the 17 variants. RT-PCR analysis was performed on RNA prepared from cultures grown at 37°C to an OD<sub>600</sub> of 4.0 in BHI medium.

*sarA* gene in both *S. epidermidis* (19) and *S. aureus* (5, 15, 42), we decided to investigate the expression of *sarA* in the *rsbU*::IS256 insertion variant 33A. This analysis revealed that *sarA* transcription was reduced in variant 33A compared to wild-type RP62A and that a similar pattern of regulation was evident in the *rsbU* transposon mutant M15 compared to its parental strain 1457 (Fig. 6). Thus, these data suggest that decreased levels of *sarA* transcription in phenotypic variants harboring *rsbU*::IS256 insertions may also contribute to diminished levels of *ica* operon expression.

A number of studies have revealed that SarA is required for maximal expression of the two staphylococcal accessory gene regulatory promoters *agr* P2 and *agr* P3 (3, 4, 6–8, 28, 35). Transcription of *agr*P3-driven RNAPIII was also substantially reduced in the *rsbU* transposon mutant M15 and the

*rsbU*::IS256 insertion variant 33A compared to 1457 and RP62A, respectively (Fig. 6), which was consistent with the decreased levels of *sarA* expression in these strains. Thus, taken together, these data suggest that IS256 insertions at *rsbU* directly affect  $\sigma^B$  activity and accordingly *sarA* expression, which in turn is associated with reduced levels of RNAPIII transcription.

**Isolation and characterization of a *sarA*::IS256 insertion variant.** To investigate the possibility that IS256 insertions at other sites may also play an important role in the production of biofilm-negative variants with diminished *ica* operon expression, we used PCR to amplify the *sarA* locus in all 43 RP62A variants that we had previously characterized (see above). One

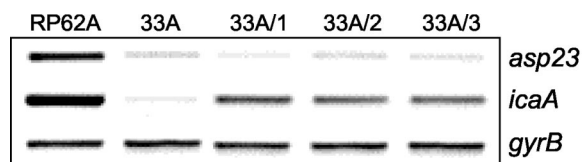


FIG. 5. Comparative measurement of *asp23*, *icaA*, and *gyrB* (control) transcription in wild-type RP62A, biofilm-negative variant 33A and three revertants from 33A. RT-PCR analysis was performed on RNA prepared from cultures grown at 37°C to an OD<sub>600</sub> of 4.0 in BHI medium.

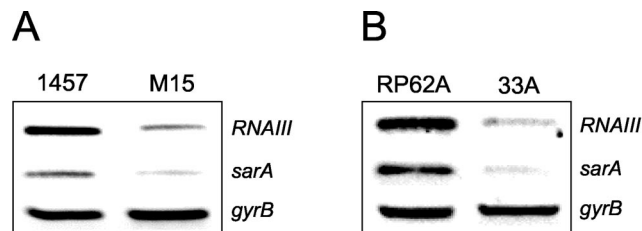


FIG. 6. Comparative measurement of RNAPIII, *sarA*, and *gyrB* (control) transcription in 1457 and M15 (A) and RP62A and 33A (B). RT-PCR analysis was performed on RNA prepared from cultures grown at 37°C to an OD<sub>600</sub> of 4.0 in BHI medium.

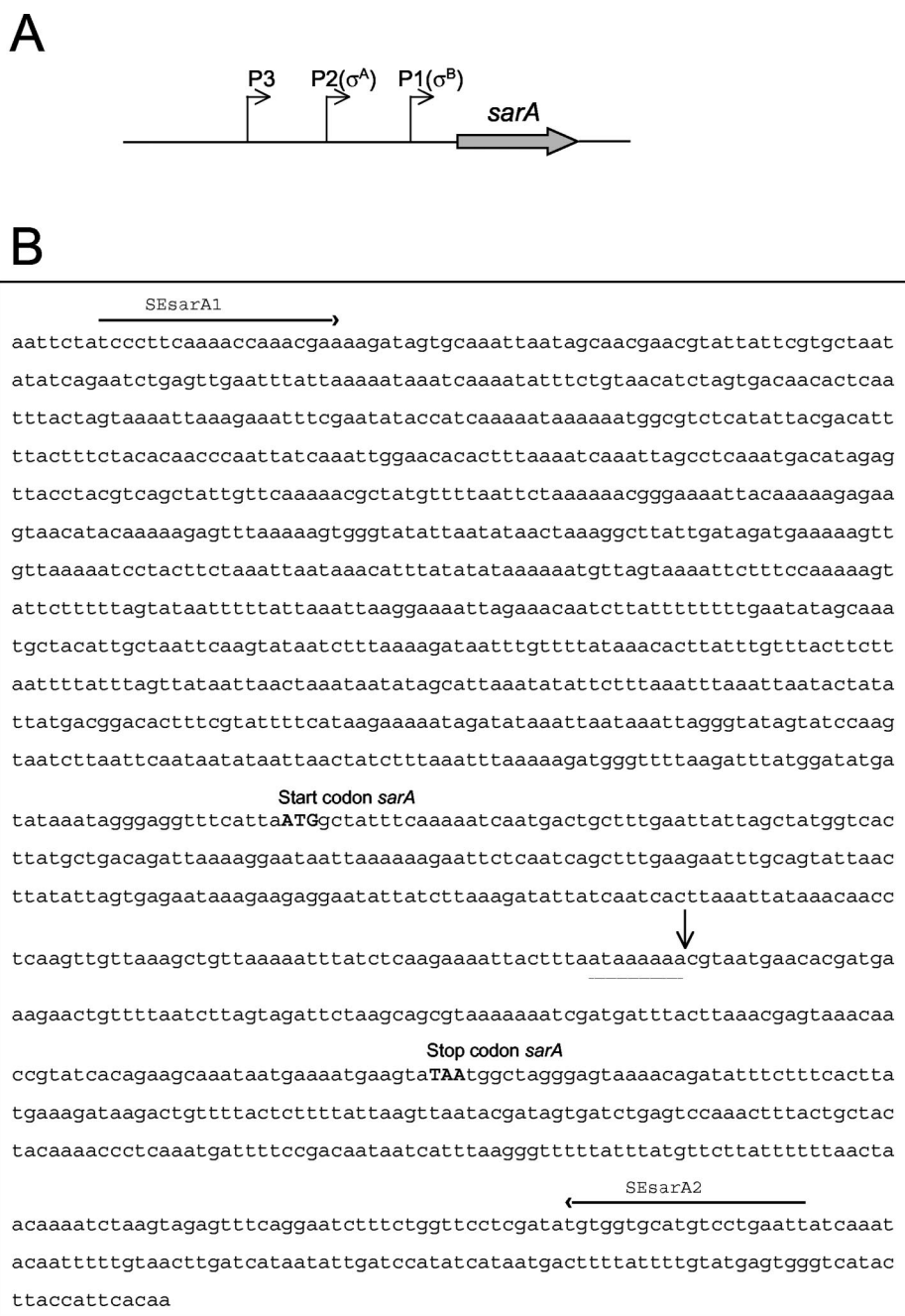


FIG. 7. Location of IS256 insertion in the *sarA* gene. (A) Diagrammatic representation of the *sarA* open reading frame and triple promoter regulatory region in *S. epidermidis*. The P1 promoter has homology to  $\sigma^B$ -dependent promoters, whereas P2 appears to be  $\sigma^A$  dependent (19). (B) Exact location of the IS256 insertion detected in the *sarA* gene of RP62A variant Red S1. The nucleotide binding sites for the PCR primers SEsarA1 and SEsarA2 and the *sarA* start and stop codons are indicated. The duplicated 8-bp IS256 target sequence, ATAAAAAA, for Red S1 is underlined, and an arrow indicates the exact insertion site.

variant, designated Red S1, was identified in which the amplified *sarA* fragment was ca. 2,800 bp compared to the expected 1,498-bp fragment produced by the wild-type RP62A. Restriction enzyme and nucleotide sequence analysis subsequently confirmed the presence of an IS256 insertion within the *sarA* gene in variant Red S1 (Fig. 7). The IS256 element was oriented in the same transcriptional orientation to the *sarA* gene and, as observed in the *rsbU*::IS256 insertion variants (Fig. 3),

was flanked by an 8-bp duplicated target sequence (Fig. 7). Interestingly, the RP62A *sarA*::IS256 insertion mutant showed a bright red, smooth colony morphology phenotype compared to the darker color of the *rsbU*::IS256 variants on CRA.

RT-PCR analysis revealed a reduction in *ica* operon transcription in the *sarA*::IS256 mutant compared to wild-type RP62A, particularly during early exponential growth (Fig. 8A). Consistent with the reduced levels of *ica* operon transcription,

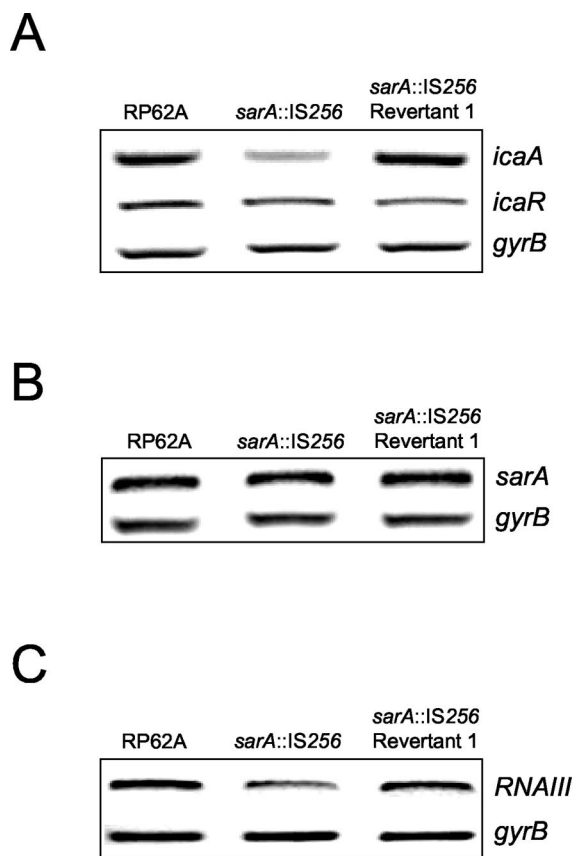


FIG. 8. Analysis of *ica* operon, *icaR*, *sarA*, and RNAIII expression in a *sarA::IS256* insertion mutant. (A) Comparative measurement of *icaA*, *icaR*, and *gyrB* (control) transcription in RP62A, Red S1 (*sarA::IS256*), and Red S1/R1 (revertant 1). RT-PCR analysis was performed on RNA prepared from cultures grown at 37°C to an OD<sub>600</sub> of 2.0 in BHI medium. (B) Comparative measurement of *sarA* and *gyrB* (control) transcription in RP62A and Red S1 (*sarA::IS256*) and Red S1/R1 (revertant 1). RT-PCR analysis was performed on RNA prepared from cultures grown to an OD<sub>600</sub> of 2.0 at 37°C in BHI medium. Primers SEsarA3 and SEsarA4, located between the *sarA* P1 promoter and the IS256 insertion site, were used to measure *sarA* transcription in the *sarA* mutant. (C) Comparative measurement of RNAIII and *gyrB* (control) transcription in RP62A, Red S1 (*sarA::IS256*), and Red S1/R1 (revertant 1). RT-PCR analysis was performed on RNA prepared from cultures grown to an OD<sub>600</sub> of 8.0 at 37°C in BHI medium.

hemagglutination assays also revealed a significant reduction in PIA/PNAG levels in the *sarA::IS256* mutant compared to RP62A (data not shown). These findings suggested that SarA is a positive regulator of *ica* operon expression in *S. epidermidis* and was consistent with the negative impact of a *sarA* mutation on *ica* operon expression in *S. aureus* (54). In contrast, decreased *ica* operon expression in the *sarA* mutant was not associated with altered regulation of *icaR* (Fig. 8A), suggesting that *icaR* expression is SarA-independent. Similarly, the IS256 insertion in *sarA* did not appear to result in altered expression of *sarA* itself, suggesting that SarA does not regulate its own transcription (Fig. 8B). Based on our earlier findings, which revealed that reduced *sarA* expression in *rsbU::IS256* insertion variants was accompanied by decreased RNAIII expression, we also examined RNAIII transcription in the *sarA::IS256* mutant. Surprisingly, this analysis only revealed no significant

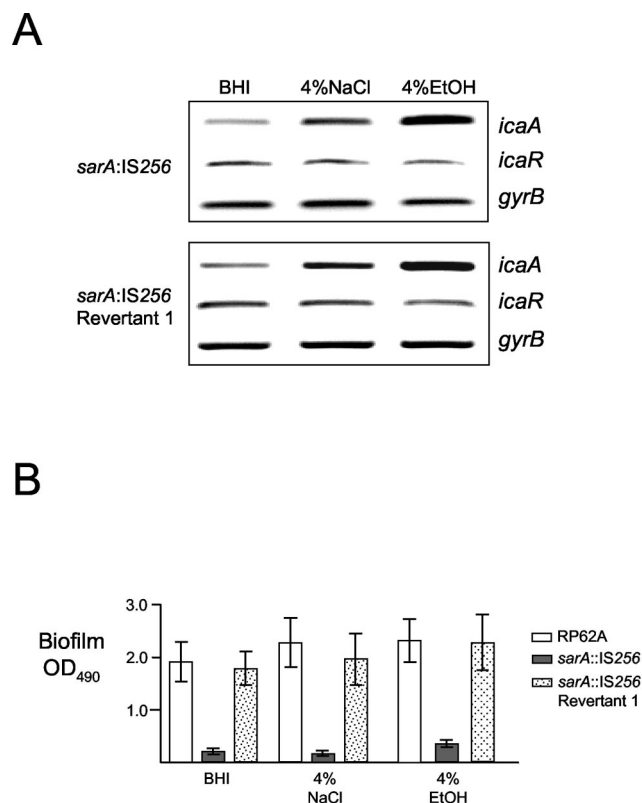


FIG. 9. Characterization of biofilm and *ica* operon environmental regulation in *S. epidermidis* RP62A, Red S1 (*sarA::IS256*) and Red S1/R1 (revertant 1). (A) Comparative measurement of *icaA*, *icaR*, and *gyrB* (control) transcription in Red S1 (*sarA::IS256*) and Red S1/R1 (revertant 1). RT-PCR analysis was performed on RNA prepared from cultures grown at 37°C to an OD<sub>600</sub> of 4.0 in BHI medium or in BHI medium supplemented with 4% NaCl or 4% ethanol. (B) Biofilm formation in tissue culture-treated 96-well plates by RP62A, Red S1 (*sarA::IS256*), and Red S1/R1 (revertant 1) in BHI medium or BHI medium supplemented with 4% NaCl or 4% ethanol. EtOH, ethanol.

difference in RNAIII expression in the *sarA* mutant compared to wild-type RP62A during early exponential growth (data not shown) and only a small reduction in RNAIII expression during early stationary growth (Fig. 8C), suggesting that *sarA* may play a more important role in the regulation of *agr* expression in *S. aureus* than in *S. epidermidis*.

Interestingly, unlike the *rsbU::IS256* mutants, a wild-type pattern of *ica* operon environmental regulation was observed in the *sarA::IS256* variant grown in NaCl or ethanol (Fig. 9A), suggesting that SarA may not be required for *ica* operon environmental regulation. However, biofilm assays revealed that ethanol- and NaCl-induced *ica* operon transcription was not accompanied by wild-type levels of biofilm-forming capacity in the *sarA* mutant (Fig. 9B), suggesting that *sarA* may also be required for normal PIA/PNAG synthesis or an *ica*-independent mechanism of biofilm formation.

Interestingly, PCR revealed a wild-type *sarA* allele (1,498-bp amplification product) in three biofilm-positive revertants isolated from the *sarA::IS256* mutant (data not shown). Nucleotide sequencing of the *sarA* locus from one revertant, Red S1/R1, revealed that IS256 had been precisely excised, leaving behind a fully intact *sarA* gene (data not shown). RT-PCR

analysis revealed that *ica* operon transcription was restored to RP62A levels in revertant Red S1/R1 (Fig. 8A). Moreover, as observed in wild-type RP62A and unlike the *sarA::IS256* insertion variant, growth of the revertant Red S1/R1 in NaCl or ethanol was associated with both *ica* operon activation and increased biofilm formation (Fig. 8).

## DISCUSSION

Staphylococcal device-related infections involving biofilms are not always localized to the site of the implanted biomaterial but are sometimes characterized by dissemination of the causative organisms and sepsis. In this context, the contribution of phase variation to the regulation of *ica* operon expression and PIA production might represent an important pathogenic mechanism facilitating the release of planktonic cells from the biofilm. In the present study we investigated the molecular basis for the production of biofilm-negative phenotypic variants with diminished *ica* operon transcription. Our data reveal that inactivation of the *rsbU* or *sarA* genes by the insertion sequence element IS256 results in diminished levels of *ica* operon transcription and is responsible for the production of ca. 11% of biofilm-negative variants in RP62A. Phenotypic variants harboring *rsbU::IS256* insertions also have impaired  $\sigma^B$  activity, as well as reduced levels of *ica*, *sarA*, and *agr* expression. Importantly, IS256 insertion mutations in the *rsbU* and *sarA* genes were also identified in biofilm-negative variants of the clinical isolate CSF24047 (data not shown), suggesting that IS256 insertion mutants may be produced by all IS256-positive strains of *S. epidermidis*. These findings are consistent with a recent report which revealed that IS256 may play a more significant role in staphylococcal virulence than other IS elements. These study demonstrated that not only was IS256 present in multiple copies on the genomes of disease-associated *S. epidermidis* strains but also that IS256 was typically associated with biofilm-forming capacity, the presence of the *ica* operon, and antibiotic resistance (33).

A direct role for IS256 in the ON-to-OFF switching of biofilm-forming capacity was initially characterized by Ziebuhr et al. (59), who demonstrated that reversible transposition of IS256 into hotspots within the *ica* operon was responsible for the production of 25 to 33% of variants. Our finding that ca. 11% of variants harbor *rsbU::IS256* insertions and that IS256 can also integrate into *sarA*, albeit at a lower frequency, reveals that this IS element is responsible for the production of up to 50% of biofilm-negative variants in *S. epidermidis* RP62A. The mechanism(s) responsible for the production of the remaining biofilm-negative variants remains unknown. However, consistent with our previous findings (25), we were able to demonstrate that up to 80% of RP62A variants have diminished levels of *ica* operon expression, indicating that this is the genetic basis for the biofilm-negative phenotype in the majority of variants produced by this strain.

In addition to the direct impact on  $\sigma^B$  activity, we also obtained evidence that the *rsbU::IS256* insertion mutation indirectly affected the expression of two global regulators: *sarA*, which is  $\sigma^B$  dependent, and *agr* (RNAIII), which is SarA dependent. These data highlight the potential of IS256, through insertions at both *rsbU* and *sarA*, to alter the global regulation of transcription and reveal that the switch to biofilm-negative is

likely to be one of multiple phenotypic changes in *rsbU* and *sarA* IS256-generated mutants. Interestingly, the absence of an identifiable  $\sigma^B$ -consensus binding site upstream of the *ica* operon (32, 51) and the observations that deletion of *sigB* does not affect biofilm development by *S. aureus* (2, 54) have led to the suggestion that  $\sigma^B$  may not directly regulate *ica* operon expression. Moreover, data which revealed that *sarA* is required for *S. aureus* *ica* operon expression and biofilm development (54) suggested that in *S. epidermidis* mutation of *sarA* or reductions in the levels of *sarA* transcription may also contribute to repression of *ica* operon expression (2). Consistent with this, analysis of the *sarA::IS256* insertion mutant revealed that SarA is directly or indirectly involved in the transcriptional regulation of *ica* operon expression. Comparative analysis of RP62A, 33A (*rsbU::IS256*), and Red S1 (*sarA::IS256*) revealed that *ica* operon transcript levels were similar in the *rsbU* and *sarA* mutants (data not shown) and may further suggest that the impact of a  $\sigma^B$  mutation on *ica* operon expression is at least in part due to decreased expression of *sarA*.

A distinctive phenotype associated with *S. epidermidis* *rsbU* mutants is the ability of ethanol but not NaCl to activate *ica* operon transcription. In contrast, both medium supplements activated *ica* operon expression in the *sarA::IS256* mutant. These findings may suggest that  $\sigma^B$  and SarA control *ica* operon expression through separate regulatory pathways. We have previously proposed that *ica* operon activation by ethanol is solely *icaR* dependent, whereas NaCl can activate *ica* expression via alterations in  $\sigma^B$  and *icaR* activity (10, 11). The data presented in the present study suggest that NaCl-induced *ica* operon activation is *sarA* independent. Interestingly, analysis of *sarA* and  $\sigma^B$  mutants in *S. aureus* revealed that PIA/PNAG levels did not reflect levels of *ica* transcription and were higher in a  $\sigma^B$ /*sarA* double mutant than in a *sarA* single mutant, suggesting that SarA and  $\sigma^B$  may compete to enhance or repress, respectively, the activity of an unknown regulatory factor involved in the synthesis or turnover of PIA/PNAG (54). Given that activation of *ica* operon expression by NaCl in the *S. epidermidis* *sarA::IS256* variant does not result in any increase in biofilm development and that ethanol-induced *ica* expression in both the *sarA* and *rsbU* mutants was not accompanied by wild-type levels of biofilm formation, it is possible that both  $\sigma^B$  and SarA are also involved in the posttranscriptional regulation of PIA/PNAG synthesis in *S. epidermidis*.

In *S. aureus*, *sarA* plays an important role in the regulation of *agr* transcription (4). However, our findings only revealed a small reduction in RNAIII expression in the *S. epidermidis* *sarA::IS256* mutant. Interestingly, although expression of the *S. aureus* and *S. epidermidis* *sarA* genes are both driven by three separate promoters, one of which is  $\sigma^B$  dependent, distinct differences possibly reflecting functional divergence between these two organisms also exist (19). For example, the *sarA* promoters are clustered much closer together in *S. epidermidis* than in *S. aureus* and as a result two small potential open reading frames (ORF3 and ORF4) that are present between the *S. aureus* *sarA* promoters are absent in *S. epidermidis* (19). Because ORF3, together with SarA protein, may play a role in regulating *agr* expression in *S. aureus* (4), it is tempting to speculate that structural differences in the *sarA* regulatory sequences may be reflected in the different effects of *sarA* mutations on RNAIII transcription in *S. epidermidis* and *S. aureus*.

A recent study by Vuong et al. (55) revealed that mutation of the *agr* locus in *S. epidermidis* was actually associated with increased biofilm-forming capacity and expression of the autolysin AtlE, which is involved in primary attachment (26), although the levels of PIA/PNAG product were not substantially affected. Similarly the recent studies of Valle et al. (54) and Beenken et al. (2) also demonstrated that mutation of *agr* did not influence biofilm forming capacity in *S. aureus*. Thus, it seems unlikely that reduced expression of RNAIII in the *sarA* and *rsbU* IS256 insertion variants is an important determinant in their biofilm-negative phenotypes.

In summary, these findings provide new insights into biofilm phenotypic variation and identify two molecular mechanisms of phenotypic switching involving insertion of a transposable element into two global regulatory genes, *rsbU* and *sarA*. These genetic switches lead not only to decreased *ica* operon transcription and impaired biofilm-forming capacity but also reduced expression of  $\sigma^B$ , *sarA*, and *agr*, which may in turn modulate the global regulation of transcription in this opportunistic bacterial pathogen. In addition, given that IS256 is highly active in multiresistant staphylococci and enterococci (36), our findings further highlight the potential of transposable elements to influence the genetic flexibility and perhaps virulence of many other important gram-positive pathogens.

#### ACKNOWLEDGMENTS

This study was funded by grants from the Research Committee of the Royal College of Surgeons in Ireland and the Irish Research Council for Science, Engineering, and Technology to J. P. O'Gara.

We are grateful to Pfizer (Ireland) for generously supporting the establishment of the RCSI Microbiology Laboratory at the RCSI Education and Research Centre. *S. epidermidis* 1457 and M15 were kindly provided by Johannes Knobloch and Dietrich Mack. Luke D. Handke and Paul D. Fey, University of Nebraska Medical Center, and Vance Fowler, Duke University, generously provided clinical isolates. We thank Ciara Kennedy, Sinead O'Donnell, Fidelma Fitzpatrick, and Tracey Dillane for experimental advice and assistance throughout the study and Charles J. Dorman for critical reading of the manuscript.

#### REFERENCES

- Baselga, R., I. Albizu, M. De La Cruz, E. Del Cacho, M. Barberan, and B. Amorena. 1993. Phase variation of slime production in *Staphylococcus aureus*: implications in colonization and virulence. *Infect. Immun.* **61**:4857–4862.
- Beenken, K. E., J. S. Blevins, and M. S. Smeltzer. 2003. Mutation of *sarA* in *Staphylococcus aureus* limits biofilm formation. *Infect. Immun.* **71**:4206–4211.
- Blevins, J. S., K. E. Beenken, M. O. Elasmri, B. K. Hurlburt, and M. S. Smeltzer. 2002. Strain-dependent differences in the regulatory roles of *sarA* and *agr* in *Staphylococcus aureus*. *Infect. Immun.* **70**:470–480.
- Cheung, A. L., M. G. Bayer, and J. H. Heinrichs. 1997. *sar* genetic determinants necessary for transcription of RNAII and RNAIII in the *agr* locus of *Staphylococcus aureus*. *J. Bacteriol.* **179**:3963–3971.
- Cheung, A. L., Y. T. Chien, and A. S. Bayer. 1999. Hyperproduction of alpha-hemolysin in a *sigB* mutant is associated with elevated SarA expression in *Staphylococcus aureus*. *Infect. Immun.* **67**:1331–1337.
- Cheung, A. L., and S. J. Projan. 1994. Cloning and sequencing of *sarA* of *Staphylococcus aureus*, a gene required for the expression of *agr*. *J. Bacteriol.* **176**:4168–4172.
- Chien, Y., and A. L. Cheung. 1998. Molecular interactions between two global regulators, *sar* and *agr*, in *Staphylococcus aureus*. *J. Biol. Chem.* **273**:2645–2652.
- Chien, Y., A. C. Manna, and A. L. Cheung. 1998. SarA level is a determinant of *agr* activation in *Staphylococcus aureus*. *Mol. Microbiol.* **30**:991–1001.
- Christensen, G. D., L. M. Baddour, B. M. Madison, J. T. Parisi, S. N. Abraham, D. L. Hasty, J. H. Lowrance, J. A. Josephs, and W. A. Simpson. 1990. Colonial morphology of staphylococci on Memphis agar: phase variation of slime production, resistance to beta-lactam antibiotics, and virulence. *J. Infect. Dis.* **161**:1153–1169.
- Conlon, K. M., H. Humphreys, and J. P. O'Gara. 2002. Regulation of *icaR* gene expression in *Staphylococcus epidermidis*. *FEMS Microbiol. Lett.* **216**:173–179.
- Conlon, K. M., H. Humphreys, and J. P. O'Gara. 2002. *icaR* encodes a transcriptional repressor involved in environmental regulation of *ica* operon expression and biofilm formation in *Staphylococcus epidermidis*. *J. Bacteriol.* **184**:4400–4408.
- Cramton, S. E., C. Gerke, N. F. Schnell, W. W. Nichols, and F. Gotz. 1999. The intercellular adhesion (*ica*) locus is present in *Staphylococcus aureus* and is required for biofilm formation. *Infect. Immun.* **67**:5427–5433.
- Cramton, S. E., M. Ulrich, F. Gotz, and G. Doring. 2001. Anaerobic conditions induce expression of polysaccharide intercellular adhesin in *Staphylococcus aureus* and *Staphylococcus epidermidis*. *Infect. Immun.* **69**:4079–4085.
- Deighton, M., S. Pearson, J. Capstick, D. Spelman, and R. Borland. 1992. Phenotypic variation of *Staphylococcus epidermidis* isolated from a patient with native valve endocarditis. *J. Clin. Microbiol.* **30**:2385–2390.
- Deora, R., T. Tseng, and T. K. Misra. 1997. Alternative transcription factor  $\sigma^{SB}$  of *Staphylococcus aureus*: characterization and role in transcription of the global regulatory locus *sar*. *J. Bacteriol.* **179**:6355–6359.
- Dunman, P. M., E. Murphy, S. Haney, D. Palacios, G. Tucker-Kellogg, S. Wu, E. L. Brown, R. J. Zagursky, D. Shlaes, and S. J. Projan. 2001. Transcription profiling-based identification of *Staphylococcus aureus* genes regulated by the *agr* and/or *sarA* loci. *J. Bacteriol.* **183**:7341–7353.
- Eisenstein, B. I. 1981. Phase variation of type 1 fimbriae in *Escherichia coli* is under transcriptional control. *Science* **214**:337–339.
- Fey, P. D., J. S. Ulphani, F. Gotz, C. Heilmann, D. Mack, and M. E. Rupp. 1999. Characterization of the relationship between polysaccharide intercellular adhesion and hemagglutination in *Staphylococcus epidermidis*. *J. Infect. Dis.* **179**:1561–1564.
- Fluckiger, U., C. Wolz, and A. L. Cheung. 1998. Characterization of a *sar* homolog of *Staphylococcus epidermidis*. *Infect. Immun.* **66**:2871–2878.
- Gerke, C., A. Kraft, R. Sussmuth, O. Schweitzer, and F. Gotz. 1998. Characterization of the *N*-acetylglucosaminyltransferase activity involved in the biosynthesis of the *Staphylococcus epidermidis* polysaccharide intercellular adhesin. *J. Biol. Chem.* **273**:18586–18593.
- Gertz, S., S. Engelmann, R. Schmid, K. Ohlsen, J. Hacker, and M. Hecker. 1999. Regulation of  $\sigma^B$ -dependent transcription of *sigB* and *asp23* in two different *Staphylococcus aureus* strains. *Mol. Gen. Genet.* **261**:558–566.
- Gertz, S., S. Engelmann, R. Schmid, A. K. Ziebandt, K. Tischer, C. Scharf, J. Hacker, and M. Hecker. 2000. Characterization of the  $\sigma^B$  regulon in *Staphylococcus aureus*. *J. Bacteriol.* **182**:6983–6991.
- Gotz, F. 2002. *Staphylococcus* and biofilms. *Mol. Microbiol.* **43**:1367–1378.
- Haldenwang, W. G. 1995. The sigma factors of *Bacillus subtilis*. *Microbiol. Rev.* **59**:1–30.
- Handke, L. D., K. M. Conlon, S. R. Slater, S. Elbaruni, F. Fitzpatrick, H. Humphreys, W. P. Giles, M. E. Rupp, P. D. Fey, and J. P. O'Gara. 2004. Genotypic and phenotypic analysis of biofilm phenotypic variation in multiple *Staphylococcus epidermidis* isolates. *J. Med. Microbiol.* **53**:367–374.
- Heilmann, C., M. Hussain, G. Peters, and F. Gotz. 1997. Evidence for autolysin-mediated primary attachment of *Staphylococcus epidermidis* to a polystyrene surface. *Mol. Microbiol.* **24**:1013–1024.
- Heilmann, C., O. Schweitzer, C. Gerke, N. Vanittanakom, D. Mack, and F. Gotz. 1996. Molecular basis of intercellular adhesion in the biofilm-forming *Staphylococcus epidermidis*. *Mol. Microbiol.* **20**:1083–1091.
- Heinrichs, J. H., M. G. Bayer, and A. L. Cheung. 1996. Characterization of the *sar* locus and its interaction with *agr* in *Staphylococcus aureus*. *J. Bacteriol.* **178**:418–423.
- Jefferson, K. K., S. E. Cramton, F. Gotz, and G. B. Pier. 2003. Identification of a 5-nucleotide sequence that controls expression of the *ica* locus in *Staphylococcus aureus* and characterization of the DNA-binding properties of IcaR. *Mol. Microbiol.* **48**:889–899.
- Jefferson, K. K., D. B. Pier, D. A. Goldmann, and G. B. Pier. 2004. The teicoplanin-associated locus regulator (TcaR) and the intercellular adhesin locus regulator (IcaR) are transcriptional inhibitors of the *ica* locus in *Staphylococcus aureus*. *J. Bacteriol.* **186**:2449–2456.
- Joyce, J. G., C. Abeygunawardana, Q. Xu, J. C. Cook, R. Hepler, C. T. Przywiecki, K. M. Grimm, K. Roper, C. C. Ip, L. Cope, D. Montgomery, M. Chang, S. Campie, M. Brown, T. B. McNeely, J. Zorman, T. Maira-Litran, G. B. Pier, P. M. Keller, K. U. Jansen, and G. E. Mark. 2003. Isolation, structural characterization, and immunological evaluation of a high-molecular-weight exopolysaccharide from *Staphylococcus aureus*. *Carbohydr. Res.* **338**:903–922.
- Knobloch, J. K., K. Bartscht, A. Sabottke, H. Rohde, H. Feucht, and D. Mack. 2001. Biofilm formation by *Staphylococcus epidermidis* depends on functional RsbU, an activator of the *sigB* operon: differential activation mechanisms due to ethanol and salt stress. *J. Bacteriol.* **183**:2624–2633.
- Kozitskaya, S., S. H. Cho, K. Dietrich, R. Marre, K. Naber, and W. Ziebuhr. 2004. The bacterial insertion sequence element IS256 occurs preferentially in nosocomial *Staphylococcus epidermidis* isolates: association with biofilm formation and resistance to aminoglycosides. *Infect. Immun.* **72**:1210–1215.
- Kullik, I., P. Giachino, and T. Fuchs. 1998. Deletion of the alternative sigma factor  $\sigma^B$  in *Staphylococcus aureus* reveals its function as a global regulator of virulence genes. *J. Bacteriol.* **180**:4814–4820.

35. Kupferwasser, L. I., M. R. Yeaman, C. C. Nast, D. Kupferwasser, Y. Q. Xiong, M. Palma, A. L. Cheung, and A. S. Bayer. 2003. Salicylic acid attenuates virulence in endovascular infections by targeting global regulatory pathways in *Staphylococcus aureus*. *J. Clin. Investig.* **112**:222–233.
36. Loessner, I., K. Dietrich, D. Dittrich, J. Hacker, and W. Ziebuhr. 2002. Transposase-dependent formation of circular IS256 derivatives in *Staphylococcus epidermidis* and *Staphylococcus aureus*. *J. Bacteriol.* **184**:4709–4714.
37. Mack, D., W. Fischer, A. Krokotsch, K. Leopold, R. Hartmann, H. Egge, and R. Laufs. 1996. The intercellular adhesin involved in biofilm accumulation of *Staphylococcus epidermidis* is a linear  $\beta$ -1,6-linked glucosaminoglycan: purification and structural analysis. *J. Bacteriol.* **178**:175–183.
38. Mack, D., M. Nedelmann, A. Krokotsch, A. Schwarzkopf, J. Heesemann, and R. Laufs. 1994. Characterization of transposon mutants of biofilm-producing *Staphylococcus epidermidis* impaired in the accumulative phase of biofilm production: genetic identification of a hexamine-containing polysaccharide intercellular adhesin. *Infect. Immun.* **62**:3244–3253.
39. Mack, D., J. Riedewald, H. Rohde, T. Magnus, H. H. Feucht, H. A. Elsner, R. Laufs, and M. E. Rupp. 1999. Essential functional role of the polysaccharide intercellular adhesin of *Staphylococcus epidermidis* in hemagglutination. *Infect. Immun.* **67**:1004–1008.
40. Mack, D., N. Siemssen, and R. Laufs. 1992. Parallel induction by glucose of adherence and a polysaccharide antigen specific for plastic-adherent *Staphylococcus epidermidis*: evidence for functional relation to intercellular adhesion. *Infect. Immun.* **60**:2048–2057.
41. Maira-Litran, T., A. Kropec, C. Abeygunawardana, J. Joyce, G. Mark III, D. A. Goldmann, and G. B. Pier. 2002. Immunochemical properties of the staphylococcal poly-*N*-acetylglucosamine surface polysaccharide. *Infect. Immun.* **70**:4433–4440.
42. Manna, A. C., M. G. Bayer, and A. L. Cheung. 1998. Transcriptional analysis of different promoters in the *sar* locus in *Staphylococcus aureus*. *J. Bacteriol.* **180**:3828–3836.
43. McKenney, D., J. Hubner, E. Muller, Y. Wang, D. A. Goldmann, and G. B. Pier. 1998. The *ica* locus of *Staphylococcus epidermidis* encodes production of the capsular polysaccharide/adhesin. *Infect. Immun.* **66**:4711–4720.
44. McKenney, D., K. Pouliot, Y. Wang, V. Murthy, M. Ulrich, G. Doring, J. C. Lee, D. A. Goldmann, and G. B. Pier. 2000. Vaccine potential of poly-1–6  $\beta$ -D-*N*-succinylglucosamine, an immunoprotective surface polysaccharide of *Staphylococcus aureus* and *Staphylococcus epidermidis*. *J. Biotechnol.* **83**:37–44.
45. Mempel, M., H. Feucht, W. Ziebuhr, M. Endres, R. Laufs, and L. Gruter. 1994. Lack of *mecA* transcription in slime-negative phase variants of methicillin-resistant *Staphylococcus epidermidis*. *Antimicrob. Agents Chemother.* **38**:1251–1255.
46. Mempel, M., E. Muller, R. Hoffmann, H. Feucht, R. Laufs, and L. Gruter. 1995. Variable degree of slime production is linked to different levels of beta-lactam susceptibility in *Staphylococcus epidermidis* phase variants. *Med. Microbiol. Immunol.* **184**:109–113.
47. Miyazaki, E., J. M. Chen, C. Ko, and W. R. Bishai. 1999. The *Staphylococcus aureus* *rsbW* (orf159) gene encodes an anti-sigma factor of SigB. *J. Bacteriol.* **181**:2846–2851.
48. O'Gara, J. P., and C. J. Dorman. 2000. Effects of local transcription and H-NS on inversion of the *fim* switch of *Escherichia coli*. *Mol. Microbiol.* **36**:457–466.
49. Petersohn, A., J. Bernhardt, U. Gerth, D. Hoper, T. Koburger, U. Volker, and M. Hecker. 1999. Identification of  $\sigma^B$ -dependent genes in *Bacillus subtilis* using a promoter consensus-directed search and oligonucleotide hybridization. *J. Bacteriol.* **181**:5718–5724.
50. Piriz Duran, S., F. H. Kayser, and B. Berger-Bachi. 1996. Impact of *sar* and *agr* on methicillin resistance in *Staphylococcus aureus*. *FEMS Microbiol. Lett.* **141**:255–260.
51. Rachid, S., K. Ohlsen, U. Wallner, J. Hacker, M. Hecker, and W. Ziebuhr. 2000. Alternative transcription factor  $\sigma^B$  is involved in regulation of biofilm expression in a *Staphylococcus aureus* mucosal isolate. *J. Bacteriol.* **182**:6824–6826.
52. Rachid, S., K. Ohlsen, W. Witte, J. Hacker, and W. Ziebuhr. 2000. Effect of subinhibitory antibiotic concentrations on polysaccharide intercellular adhesin expression in biofilm-forming *Staphylococcus epidermidis*. *Antimicrob. Agents Chemother.* **44**:3357–3363.
53. Rupp, M. E., N. Sloat, H. G. Meyer, J. Han, and S. Gatermann. 1995. Characterization of the hemagglutinin of *Staphylococcus epidermidis*. *J. Infect. Dis.* **172**:1509–1518.
54. Valle, J., A. Toledo-Arana, C. Berasain, J. M. Ghigo, B. Amorena, J. R. Penades, and I. Lasa. 2003. SarA and not  $\sigma^B$  is essential for biofilm development by *Staphylococcus aureus*. *Mol. Microbiol.* **48**:1075–1087.
55. Vuong, C., C. Gerke, G. A. Somerville, E. R. Fischer, and M. Otto. 2003. Quorum-sensing control of biofilm factors in *Staphylococcus epidermidis*. *J. Infect. Dis.* **188**:706–718.
56. Vuong, C., F. Gotz, and M. Otto. 2000. Construction and characterization of an *agr* deletion mutant of *Staphylococcus epidermidis*. *Infect. Immun.* **68**:1048–1053.
57. Vuong, C., H. L. Saenz, F. Gotz, and M. Otto. 2000. Impact of the *agr* quorum-sensing system on adherence to polystyrene in *Staphylococcus aureus*. *J. Infect. Dis.* **182**:1688–1693.
58. Ziebuhr, W., C. Heilmann, F. Gotz, P. Meyer, K. Wilms, E. Straube, and J. Hacker. 1997. Detection of the intercellular adhesion gene cluster (*ica*) and phase variation in *Staphylococcus epidermidis* blood culture strains and mucosal isolates. *Infect. Immun.* **65**:890–896.
59. Ziebuhr, W., V. Krimmer, S. Rachid, I. Lossner, F. Gotz, and J. Hacker. 1999. A novel mechanism of phase variation of virulence in *Staphylococcus epidermidis*: evidence for control of the polysaccharide intercellular adhesin synthesis by alternating insertion and excision of the insertion sequence element IS256. *Mol. Microbiol.* **32**:345–356.